https://doi.org/10.2352/EI.2023.35.8.IQSP-319

Improvement of the flare evaluation for cameras and imaging applications when using near-infrared lighting

Elodie Souksava, Emilie Baudin, Claudio Greco, Hoang-Phi Nguyen, Laurent Chanas, Frédéric Guichard
DXOMARK, Boulogne-Billancourt, France

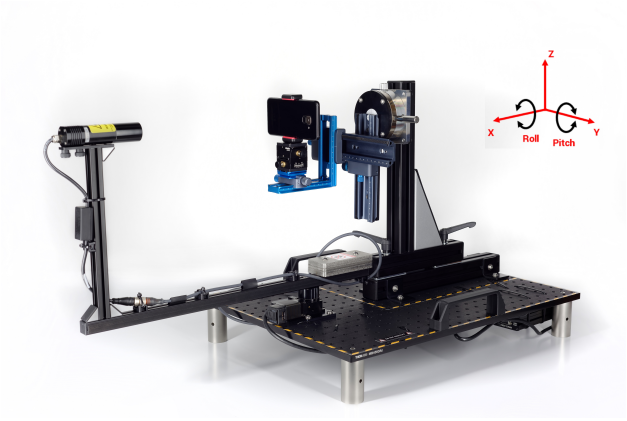

Figure 1. *DXOMARK Flare and MTF compass bench. An automated setup on 3 optical directions [3].*

Abstract

The number of cameras designed for capturing the near-infrared (NIR) spectrum (sometimes in addition to the visible) is increasing in automotive, mobile, and surveillance applications. Therefore, NIR LED light sources have become increasingly present in our daily lives. Nevertheless, camera evaluation metrics are still mainly focused on sensors in the visible spectrum.

The goal of this article is to extend our existing flare setup and objective metric [1] to quantify NIR flare for different cameras and to evaluate the impact of NIR filters on lenses. We also compare the results in both visible and NIR lighting.

Moreover, we propose a new method to measure with our flare setup the ISO speed rating in the visible spectrum (as originally defined in ISO standard 12232 [2]) as well as an equivalent sensitivity defined for the NIR spectrum.

Introduction

Current flare evaluation metrics are mainly used to evaluate cameras in the visible spectrum. In our previous work [1], we proposed a complete hardware and software flare measurement protocol. The flare setup (Figure 1) allows to evaluate the flare with a collimated light source, for any orientation on three axes and any position in and out of the field of view (FOV) of the device. The measurement protocol defines the procedure to find the exposure time that maximises the measurement accuracy without saturating the flare image, whether the source is in the FOV of the camera or not. When the source is in the FOV of the camera, the flare inside the collimator lens of the source is not included in the measurement.

The aim of the flare measurement is to quantify the lens flare. It works on RAW images to ensure the linearity between the pixels value and the illuminance received by the sensor. The flare attenuation, expressed in decibel (dB), is the ratio between the source illuminance E_s, *i.e.*, the illuminance received at the location of the device under test, and the flare illuminance E_f, i.e. the virtual illuminance of a scene that would generate the same response on the sensor as the flare, both expressed in lux. Note that since the illuminance is homogeneous to a power, in flare attenuation we use a definition of dB based on $10 \cdot \log_{10}$, which needs to be considered when comparing the flare attenuation to the SNR or the dynamic range.

$$Flare_{att} = 10 \cdot \log_{10}\left(\frac{E_s}{E_f}\right) \tag{1}$$

NIR light sources and sensors are more and more common for different camera use cases: time-of-flight (ToF) cameras, lidar cameras, surveillance cameras, automotive cameras, *etc*. As NIR wavelengths are invisible to the human eye, IR lightings are used to enhance security camera performance in night time without disturbing and causing light pollution. Nowadays, the most used wavelengths for NIR sources are 850 nm and 940 nm. However, 850 nm lights can produce a slight red glow visible to human eye and some cameras are not sensitive enough at 940 nm.

The aim of our work is to extend our existing flare measurement and protocol to cameras in the NIR spectrum. This will allow us to compare the performance of cameras designed to capture NIR light as well as visible light cameras designed to suppress or attenuate it with IR filters. To achieve this, it was important to have new light sources emitting in NIR light that are adapted to our existing setup. This will allow to compare visible and NIR flare results with the same flare setup.

Since the ISO speed rating is used in the flare metric and is defined for visible lights [2], one of the main work was to find an analogous of the ISO speed rating in the NIR spectrum.

Our flare setup and metric are now able to quantify flare for both visible and NIR lights. We can evaluate flare on NIR cameras, but also test the performance of NIR filters on visible cameras. Moreover, our flare setup enables us to compute the ISO speed rating with a visible source or an equivalent sensitivity with an NIR source.

Flare theory

Flare measurement with a collimated light source

The flare has been defined as glare spread function (GSF) in the standard ISO 9358:1994 [4]. We consider a light source at

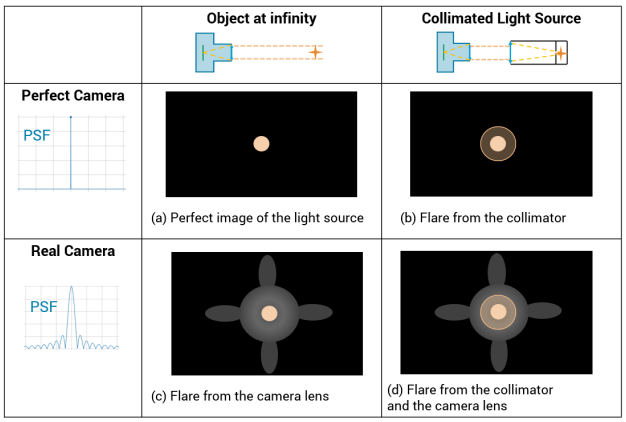

Figure 2. *Perfect vs real system*

infinity with an apparent size α, and a camera focused at infinity with the light source in the center of the FOV. Note that the GSF is related to the point spread function (PSF) for a point source. In that case, flare image is the convolution of the perfect image of the light source with the GSF. The differences are that the GSF is defined only outside of the geometric image of the source, and that the GSF is larger compared to the PSF, but with a very low value compared to the PSF.

With a perfect camera, i.e. without aberration and diffraction, focused at infinity, the PSF (or GSF) is a dirac pulse, and the image of the light source is a disk and its size depends on the apparent size of the light source and the focal length of the camera (Fig. 2(a)). With a real camera with non-perfect PSF, the image presents a figure of flare, which is the convolution of the PSF with the perfect image of the source (Fig. 2(c)).

The best way to get a light source at infinity is through a collimator. In this case, the light source is not perfect anymore. The collimator optic can produce flare, and there can be reflections inside the collimator tube. By design, all the reflections and flare of the collimator lens will be viewed inside the image of the collimator front lens by the perfect camera (Fig. 2(b)). With the real camera, the light source image is convoluted with the PSF. The figure of flare is the same as before, with the flare and reflections from the collimator, but they are very small compared to the flare image of the source itself (Fig. 2(d)).

When evaluating a camera, we want to measure the flare from the camera only. From the flare measurement, we want to exclude the image of the collimator including reflections and flare in the collimator lens, for which we have defined a protocol [1]. We use the assumption that the total dynamic of the flare image is larger than the dynamic of the sensor. If we want good measurement precision in the darkest parts of the image, the image of the light source and the pixels around it will always be saturated. These saturated pixels have to be removed from the flare measurement. We choose to remove also all the pixels inside the area of the collimator tube, after making sure that there are no saturated pixels in the rest of the image.

In practice, we need to choose an exposure time long enough to have a good measurement precision, but short enough so there are no saturated pixels outside of the collimator tube (see Figure 3). The ideal exposure is when all pixels inside the collimator tube are saturated, and no pixel is saturated outside of it, though

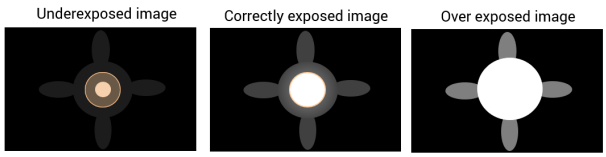

Figure 3. *Exposure*

it is not always possible to find such an exposure time.

The same applies for any position of the light source in the FOV of the camera. When the light source is not in the FOV of the camera, we do not need to remove any pixels from the image, and we can usually use larger exposure times as long as the flare image is not saturated.

Link between the flare metric and the GSF

The illuminance received on the sensor E_r is the convolution of the image of a perfect light source $E_{s'}$ with the normalized GSF:

$$E_r(x,y) = (GSF * E_{s'})(x,y) \tag{2}$$

We assume perfect lenses and that the collimated source and the camera are aligned on the same optical axis (see Figure 4). The total flux Φ_c of the image of the source will be the same received by the front lens of the camera:

$$\Phi_c = \frac{\pi E_s D_c^2}{4} \tag{3}$$

with D_c the diameter of the camera lens and E_s the source illuminance received in front of the lens. In the case when the image of the source is small compared to a pixel, we can write for each pixel:

$$E_r(x,y) = GSF\,\frac{\pi E_s D_c^2}{4} \tag{4}$$

Considering the flare metric in linear scale without the log computation $Flare_m$, we have:

$$Flare_m(x,y) = \frac{E_s}{E_f(x,y)} \tag{5}$$

with E_f the virtual illuminance of a white lambertian surface that will give the measured grey level received by the sensor. So we have $E_f = \pi L_f = 4A^2 E_r$, with $A = \frac{f_c}{D_c}$ the F-number of the camera lens and f_c the focal length of the camera. Finally, we have:

$$Flare_m(x,y) = \frac{E_s}{4A^2 E_r} = \frac{E_s}{A^2 GSF(x,y)\pi E_s D_c^2} = \frac{1}{GSF(x,y)\pi f_c^2} \tag{6}$$

From these results, we can conclude that the flare metric depends on the GSF and the focal length of the camera but it does not depend on the lens optical design of the collimator.

Sensitivity measurement

In our previous work [1] we used the ISO speed rating [2] to measure the flare virtual illuminance E_f, the amount of flare received by the sensor. However, in practice, it may not be easy to

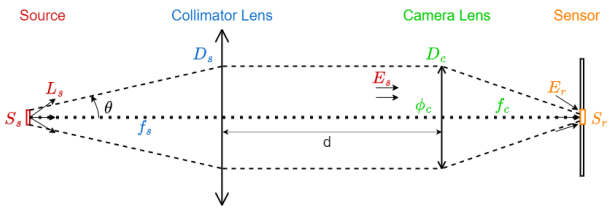

Figure 4. *Radiometry for the full optical path : collimator and camera*

measure the sensitivity of a sensor, which requires another setup. For this reason, we provide the theoretical analysis to convert the flare metric from photometric to radiometric units for the NIR spectrum. Furthermore, we introduce here an easier method that works on our flare bench.

We assume that camera sensors are linear with the received light as long as they are not saturated, therefore we can write the relation between the linearized gray levels $x = (\text{grayLevel} - \text{darkLevel})$ of any RAW image and the luminance L in a visible scene, knowing the aperture A and the exposure time t, with respect to a constant K:

$$x = K \cdot \frac{t \cdot L}{A^2} \tag{7}$$

K can be measured on any image with a known linearized gray level x_0 and known luminance L_0 and exposure time t_0:

$$K = x_0 \cdot \frac{A^2}{t_0 \cdot L_0} \tag{8}$$

To measure x_0, we need a uniform lambertian surface, large enough to be accurate when computing statistics in the image of the device under test (DUT). For ease and speed, we found a way to measure it with the same setup by adding a diffuser in front of the collimated light source. The diffuser used will avoid the blooming of the source and allow to generate a lambertian uniform patch of luminance L_0 at the center of the image. We choose an exposure time t_0 for the camera so that the uniform patch is not saturated. An example of valid captured image is presented in the Figure 5. Then, x_0 can be computed as the average linearized gray level value on the uniform patch, and equation (7) can be written as:

$$L = L_0 \cdot \frac{t_0}{t} \cdot \frac{x}{x_0} \tag{9}$$

Note that the F-number A has been simplified out of the equation. We now consider a flare image, with $x = x_f$, $t = t_f$ and $L = L_f$. We can simplify the computation of E_f in the flare measurement equation (1) with:

$$\begin{aligned} E_f &= \pi \cdot L_f \\ &= \pi \cdot L_0 \cdot \frac{t_0}{t_f} \cdot \frac{x_f}{x_0} \end{aligned} \tag{10}$$

Flare measurement for NIR applications

NIR lighting

We have selected two new NIR sources to complete our flare setup: one at 850 nm and one at 940 nm. These are the most commom wavelengths used in NIR cameras illuminators to enhance security camera performance in night time.

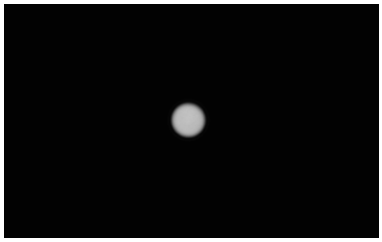

Figure 5. *Uniform non-saturated gray level patch with x_0, t_0 and L_0 the luminance of the source with the diffuser in front.*

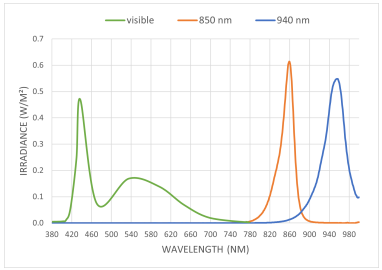

Figure 6. *Spectrum of the visible and NIR sources.*

Moreover, the emission of the sun in NIR is more than half of what is emitted in the visible spectrum. So, devices intended for visible capture that are not properly blocking the NIR spectrum may capture unwanted signal due to NIR emission.

Our current visible light source is an LED with a luminance around 5.4×10^7 cd/m^2 comparing to the luminance of the sun that is 1.6×10^9 cd/m^2 at noon, and with a limited emission above 700 nm. This means that we cannot evaluate visible or NIR cameras performances to detect any flare in NIR spectrum.

Thus, we complete our existing flare setup with new collimated NIR sources at 850 nm and 940 nm, in addition to the visible source. The spectra of the three light sources are presented on Figure 6. The new sources have the same tube diameter of 25 mm as the visible source, with an apparent diameter of 0.88°.

Flare measurement for NIR

We can measure the flare using a light source with any spectrum as long as we measure the radiance L_0 using the same source or with the exact same spectrum distribution. In the NIR bandwidth, the two values E_s and E_f in the flare formula (1) become irradiance values expressed in W/m^2, but that does not change the unit of the flare attenuation in dB.

Photometric		Radiometric	
Quantity	**Units**	**Quantity**	**Units**
Luminous Power	lm = cd·sr	Radiance Power	W
Luminance	cd/m^2	Radiance	W/m^2/sr
Illuminance	lux = lm/m^2	Irradiance	W/m^2

Figure 7. *Summary of the photometric and radiometric quantity [5]*

As the flare measurement does not depend on the ISO speed value, as demonstrated in the equation (10), which is only defined in the visible bandwidth, we can now extend the flare measurement to the NIR spectrum. We can also compute the equivalent sensitivity measurement in NIR spectrum by using radiometric units instead of photometric units (see Figure 7).

However, the first diffuser we used in front of the light source to have a uniform patch to compute x_0 in the equation (10) is not lambertian near IR transmission. As we can see in the Figure 8(a), the NIR LED is visible despite the first diffuser in front of the collimated source. It was therefore necessary to find a new diffuser lambertian in both visible and NIR bandwidth to have a uniform patch for both sources. The Figures 8(b) and 8(d) show that the new diffuser is lambertian and allows to have a uniform patch with the NIR source, as in the visible spectrum, to compute a gray level non saturated and to compute E_f from the equation (10).

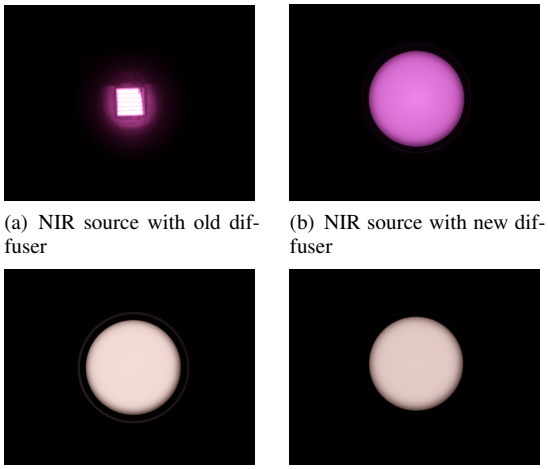

(a) NIR source with old diffuser

(b) NIR source with new diffuser

(c) Visible source with old diffuser

(d) Visible source with new diffuser

Figure 8. *Diffusers on the visible and NIR sources*

Results

Flare Measurement results

Tests have been performed with an automotive camera on a visible light source and a 940 nm NIR light source, on the horizontal axis. Two lenses with the same optical design for the visible spectrum have been tested. However, one of the lenses includes an IR cut-off filter and the other does not. The goal of these tests is to see if the flare is impacted by the presence of the IR cut-off filter on the lens and to compare the results with the visible and NIR sources.

The first observation we can do on Figure 9 is that the NIR light source generates more flare for both lenses. As a reminder, a low attenuation value means that a large amount of unwanted light arrives to the sensor, resulting in poor image quality.

With the visible source, we can see that there is more flare for the lens with the IR cut-off filter. The IR filter is adding more flare especially when the source starts to be out the FOV at 31° from the center. We can see on the flare attenuation map in the Figures 10(a) and 10(b) that with the visible source the figure of flare is stronger for the lens with the IR cut-off filter than the lens without the IR filter at 37°.

Regarding the NIR source, the flare is more visible when using the lens without the IR cut-off filter. We can see on the Figure 10 at 0° position that the figure of flare for the two lenses is different. For the lens without the IR cut-off filter the figure of flare is circular around the NIR light source as we can see in the Figure 10(d), which corresponds to the lens flare. Whereas for the other lens, the IR filter creates some petal shape flare around the light source, as shown in the Figure 10(c). We can say that in our case with the 940 nm NIR source, the amount of flare is lower by having a filter on the lens, but the filter can add flare figures, different from the optical flare when the source is in the FOV.

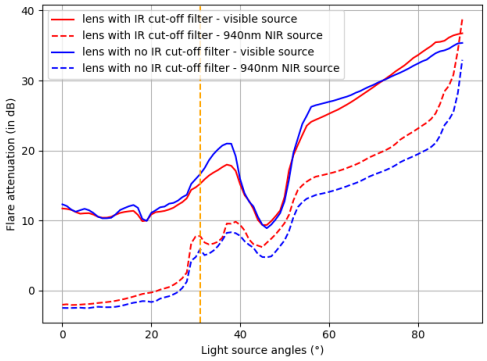

Figure 9. *Comparison of the flare attenuation average metric on both lenses 1 and both sources.*

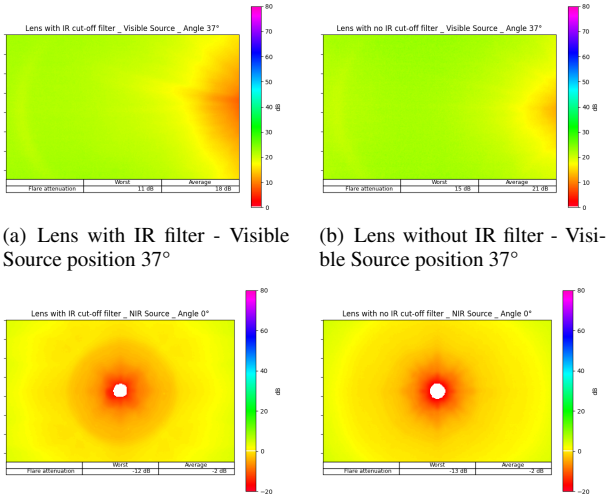

(a) Lens with IR filter - Visible Source position 37°

(b) Lens without IR filter - Visible Source position 37°

(c) Lens with IR filter - NIR Source position 0°

(d) Lens without IR filter - NIR Source position 0°

Figure 10. *Comparison between the two lenses with the visible source at 37° and the NIR source at 0°.*

Flare in a natural scene

In the previous sections, we have explained how to accurately measure the flare for visible and NIR light sources. In this section we will show how they relate to a real scene, and how we can use the flare map to simulate the flare in natural images with the visible light source.

We consider a scene where a light source, for example the sun, illuminates uniformly the scene. The DUT is framing the uniformly illuminated scene, and at the same time it receives lighting from this source, which generates lens flare. In this case, the illuminance received at the front of the DUT is the same as the illuminance of the scene. A corresponding lab setup is visible in Figure 11(a). We have used a DXOMARK DMC chart, uniformly

illuminated with the Automated Lighting System (ALS) in D65. The direct lighting is represented by the flare visible light source. The illuminance on the chart from the ALS, and the illuminance on the DUT from the flare source are the same: 13000 lux. Figure 11(b) shows the captured image from this lab scene, with the flare source at 48°, outside of the device FOV. We can see a strong flare figure on the side of the image, that reduces the contrast.

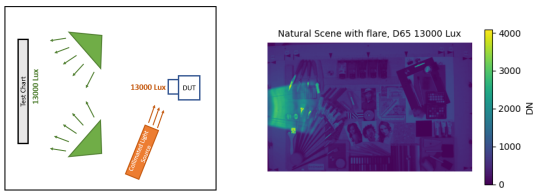

(a) Lab setup (b) Captured Image

Figure 11. *Lab setup reproducing a real scene with flare, and captured image (D65 13000 Lux, flare source oriented at 48°)*

We now introduce a method to simulate this result from the flare attenuation map and any natural image. Here we use an image of the same natural scene as before (Figure 12(a)). We can use equations (1) and (10) to compute the equivalent flare gray levels from known illuminance received on the scene and the flare attenuation map (Figure 12(b)). We can then add them to the original image and get a simulated image with flare, visible on Figure 12(c). We can see that the simulated image looks very similar to the captured image from Figure 11(b). This confirms that this method allows to use the results from our flare measurement to simulate the flare in natural images.

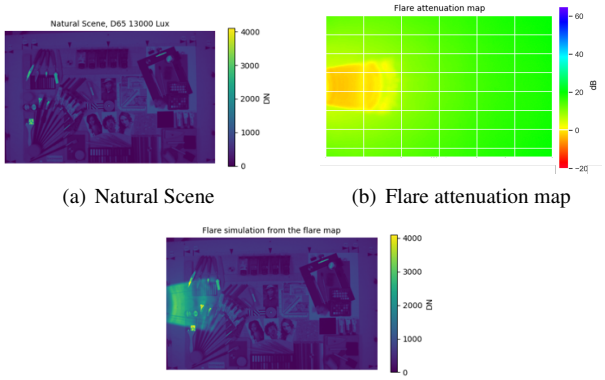

(a) Natural Scene (b) Flare attenuation map

(c) Simulated Image with Flare

Figure 12. *Flare simulation from the flare attenuation map in a D65 13000 Lux natural scene*

Conclusion and future work

Our work has led to the integration of the computation of the ISO speed measure in the flare formula. Knowing that it may be difficult to compute the sensitivity of the sensor, we proposed a new protocol to compute it directly with our flare setup.

In addition to the visible spectrum, we have extended our flare measurement in the NIR spectrum with new NIR sources at 850 and 940 nm. This new improvement in the measure allows us to test our protocols with the new NIR light sources. Moreover, we were able to evaluate and compare the performance of two lenses that only differ by the presence or absence of IR cut-off filter. Our setup allowed us to analyze the behavior of the IR cut-off filter on the flare with the visible and NIR light sources. We observed different behaviors with both light sources. More information from suppliers about the filter would be needed to correlate the results.

The next possible improvements for our setup would be to have a source that is emitting both in the visible and in a broader NIR spectrum to simulate closer to the sun spectrum.

References

[1] E. Souksava, T. Corbier, Y. Li, F.-X. Thomas, L. Chanas, and F. Guichard, "Evaluation of the lens flare," *Electronic Imaging*, vol. 33, pp. 1–7, 2021.

[2] ISO 12232:2019, "Photography — digital still cameras — determination of exposure index, iso speed ratings, standard output sensitivity, and recommended exposure index," *Standard, International Organization for Standardization*, 2019.

[3] DXOMARK, "Analyzer flare & mtf (compass setup)." https://corp.dxomark.com/analyzer-flare-mtf-compass-setup, 2022.

[4] ISO 9358:1994, "Optics and optical instruments — veiling glare of image forming systems — definitions and methods of measurement," *Standard, International Organization for Standardization*, 1994.

[5] J.-L. Meyzonette and T. Lépine, *Bases de radiométrie optique*. Cépaduès-Éditions, 2 ed., 2001.